IOSR Journal of Applied Physics (IOSR-JAP)
e-ISSN: 2278-4861.Volume 6, Issue 2 Ver. II (Mar-Apr. 2014), PP 15-21
www.iosrjournals.org

The electronic band parameters calculated by the Tight Binding Approximation for $Cd_{1-x}Zn_xS$ quantum dot superlattices

S. Marzougui, N. Safta
Unité de Physique Quantique, Faculté des Sciences, Université de Monastir, Avenue de l'Environnement, 5000 Monastir – Tunisia.

Abstract: *This work reports on a theoretical study of superlattices based on $Cd_{1-x}Zn_xS$ quantum dots embedded in an insulating material. This system, assumed to a series of flattened cylindrical quantum dots with a finite barrier at the boundary, is studied using the tight binding approximation. The electronic states of Γ_1 – miniband have been computed as a function of zinc composition for different inter-quantum dot separations. Calculations have been made for electrons, heavy holes and light holes. Three main features were revealed: (i) in the case of electrons, the Zn composition x = 0.4 is expected to be the most favorable to give rise a superlattice behavior for the $Cd_{1-x}Zn_xS$ quantum dots studied (ii) the strong localization character of heavy holes is evident in the $Cd_{1-x}Zn_xS$ nanostructures (iii) the $Cd_{0.2}Zn_{0.8}S$ system is the more appropriate to exhibit a superlattice behavior for light holes especially when the superlattice period is low.*

Keywords: *Quantum dots, superlattices, $Cd_{1-x}Zn_xS$, Tight Binding Approximation, non volatile memories.*

I. Introduction

From the fundamental viewpoint, the study of electronic and optical properties quantum dots (QDs) based on the $Cd_{1-x}Zn_xS$ ternary alloy is attracting a considerable interest. This is mainly due to their specific characteristics like size quantization, zero – dimensional electronic states, non linear optical behaviour… [1-8]. On the subject of the growth methods used to prepare $Cd_{1-x}Zn_xS$ QDs, we can cite the inverted micelles [9], the selective area – growth technique [10], the single source molecular precursors [11], the colloidal method [12] and the Sol gel technique [1].

Concerning the nanostructure devices design, one of the most prominent topics is to use nanostructures containing tunneling – coupled QDs as an active element. In this framework, we have made some theoretical investigations of superlattices based on $Cd_{1-x}Zn_xS$ quantum dots embedded in an insulating material [13-17]. To describe the QDs, we have adopted the flattened cylindrical geometry with a finite potential barrier at the boundary. In Ref [14], we have used the Kronig-Penney model to illustrate the confinement potential. Thus, we have calculated the ground and the first excited minibands for both electrons and holes. We have also computed the longitudinal effective mass. Calculations were carried out as a function of the Zn composition and the inter-quantum dot separation. In Ref [15], we have used the sinusoidal potential to model the confinement of the carriers. Within this model, we have studied the ground and the first excited minibands for electrons as a function of inter-quantum dot separation for different zinc compositions. In Ref [16], using the triangular potential model, we have calculated, for electrons, heavy holes and light holes, the Γ_1 – miniband and the longitudinal effective mass versus the Zn composition and the inter-quantum dot separation as well.

The goal of the present work is to investigate systematically the coupling in superlattices made by $Cd_{1-x}Zn_xS$ QDs having a flattened cylindrical geometry with a finite potential barrier at the boundary. Calculations have been carried out as a function of Zn composition going from CdS to ZnS using the Tight Binding Approximation (TBA). The paper is organized as follows: after a brief introduction, we present the theoretical formulation, in the following we report the numerical results obtained, conclusions derived from this study are given in the last section.

II. Theoretical Formulation

In a realistic description, the electronic properties of $Cd_{1-x}Zn_xS$ QDs embedded in a dielectric matrix have to be studied theoretically using spherical geometry. Based on this model, two methodologies have been proposed to describe the potential energy, a potential with an infinite barrier [1-3, 18, 19] and a potential with a finite barrier [7, 8] at the boundary. The latter potential has the advantage to consider the coupling between QDs. Nevertheless, it presents a big difficulty concerning the determination of the band edges for coupled QDs.

Fig. 1- a shows the geometry used to describe a chain of $Cd_{1-x}Zn_xS$ QDs. The common confined direction is denoted by z. The inter-quantum dot separation is labelled d which corresponds to the period of the structure. Along a common direction of spherical $Cd_{1-x}Zn_xS$ QDs, electrons and holes see a succession of flattened cylinders of radius R and effective height L. According to that reported in Ref [1], the diameter D = 2R

varies from 9 nm to 4 nm going from CdS to ZnS. Thus, if we consider L = 1 nm which corresponds to the value reported in Ref [13], one can note that L is lower than D and therefore the quantum confinement along transversal direction can be disregarded. Consequently, the $Cd_{1-x}Zn_xS$ multi – quantum dot system being studied can be considered as a QDs superlattice along the longitudinal confined direction. Thus, the system to investigate is a $Cd_{1-x}Zn_xS$ QD superlattice where the $Cd_{1-x}Zn_xS$ flattened cylinders QDs behave as wells while the host dielectric lattice forms a barrier of height U_0. For the sake of simplicity, the electron and hole states are assumed to be uncorrelated. The problem to solve is, then, reduced to those of one particle in a one dimensional potential. In this work, we consider the potential depicted in **Fig. 1- b**. Such a potential can be expressed as:

$$V_{e,h}(z) = \sum_n U_{e,h}(z - nd) \quad \textbf{(1)}$$

with

$$U_{e,h}(z) = \begin{cases} 0; -L/2<z<L/2 \\ U_{0e,h}; L/2<z<d-L/2 \end{cases}$$

The subscripts *e* and *h* refer to electrons and holes respectively and n is the nth period. For this potential, the electron and hole states can be calculated using the effective Hamiltonian:

$$H_{e,h} = \frac{-\hbar^2}{2m^*_{e,h}} \frac{d^2}{dz^2_{e,h}} + V_{e,h}(z_{e,h}) \quad \textbf{(2)}$$

where $\hbar$ is the Plank's constant and m^* is the effective mass of carriers. In deriving the Hamiltonian $H_{e,h}$, we have adopted the effective mass theory (EMT) and the band parabolicity approximation (BPA). The mismatch of the effective mass between the well and the barrier has been neglected. Values of the electron and hole effective masses, as adopted for CdS and ZnS [14,17], are listed in Table 1. These two parameters for $Cd_{1-x}Zn_xS$ with different Zn compositions have been deduced using the Vegard's law.

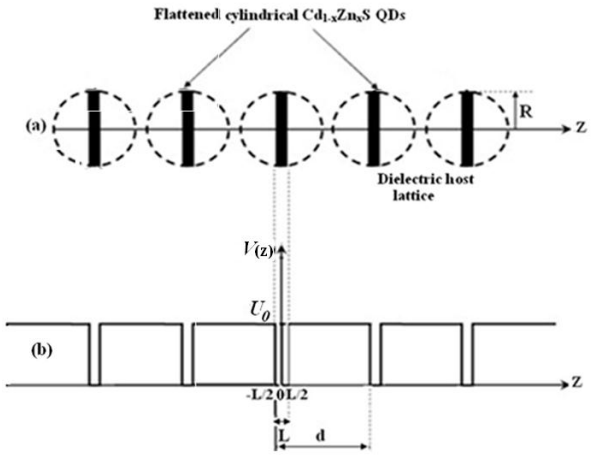

Fig.1: (a) A schematic diagram of $Cd_{1-x}Zn_xS$ QD superlattices according to the flattened cylindrical geometry – (b) The barrier potential in the framework of the Tight Binding Approximation.

We have resolved the Schrodinger equation using the Tight Binding Approximation. Our calculation shows that the Γ_1 – miniband width is given by:

$$\Delta E_{1e,h} = 4\beta_{e,h} \quad \textbf{(3)}$$

where

$$\beta_{e,h} = U_{0e,h}\left[(d-L)\, B_{e,h}{}^2\, e^{-\rho_{e,h}(d-L)} + \frac{B_{e,h}{}^2\, e^{-\rho_{e,h} d}}{\rho_{e,h}} + \frac{2A_{e,h}B_{e,h}\, e^{-\rho_{e,h}\left(d-\frac{L}{2}\right)}}{\rho_{e,h}{}^2 + k_{e,h}{}^2}\left(\rho_{e,h}\cos\left(\frac{k_{e,h}L}{2}\right)sh\left(\frac{\rho_{e,h}L}{2}\right) + k_{e,h}\sin\left(\frac{k_{e,h}L}{2}\right)ch\left(\frac{\rho_{e,h}L}{2}\right)\right)\right] \quad \textbf{(4)}$$

with

$$A_{e,h} = \left[\frac{L}{2} + \frac{\cos^2\left(\frac{k_{e,h}L}{2}\right)}{\rho_{e,h}} + \frac{\sin(k_{e,h}L)}{2k_{e,h}} \right]^{-\frac{1}{2}} \quad \textbf{(5)}$$

$$B_{e,h} = A_{e,h}\cos\left(\frac{k_{e,h}L}{2}\right) \quad \textbf{(6)}$$

$$k_{e,h} = \sqrt{\frac{2m^*_{e,h}E_{1e,h}}{\hbar^2}} \quad \textbf{(7)}$$

$$\rho_{e,h} = \sqrt{\frac{2m^*_{e,h}\left(U_{0e,h} - E_{1e,h}\right)}{\hbar^2}} \quad \textbf{(8)}$$

Here, E_{1e} corresponds to the lowest energy of electrons, E_{1hh} is the lowest energy of heavy holes and E_{1lh} is the lowest energy of light holes. All these energies are associated with an isolated flattened cylindrical quantum dot of $Cd_{1-x}Zn_xS$.

III. Results

In a first phase, we have calculated, for electrons, the width ΔE_{1e} of the Γ_1 −miniband as a function of the ZnS molar fraction. Values of parameters used in these calculations are summarized in Table 1. All these parameters are taken from Refs [14, 17].

Table. 1: Parameters used to calculate the Γ_{1e} - , Γ_{1hh} - and Γ_{1lh} - minibands for $Cd_{1-x}Zn_xS$ QD superlattices.

X	$\frac{m^*_e}{m_0}$	$\frac{m^*_{hh}}{m_0}$	$\frac{m^*_{lh}}{m_0}$	$U_{0e}\ (eV)$	$U_{0h}\ (eV)$	$L\ (nm)$	$E_{1e}(eV)$	$E_{1hh}(eV)$	$E_{1lh}(eV)$
0.0	0.16	5.00	0.70	0.10	0.25	1.0	0.090	0.040	0.129
0.2				0.25	0.25	1.0	0.187	0.049	0.136
0.4				0.45	0.50	1.0	0.292	0.060	0.216
0.6				0.75	0.50	1.0	0.384	0.070	0.238
0.8				1.50	0.50	1.0	0.531	0.083	0.266
1.0	0.28	1.76	0.23	2.00	2.00	1.0	0.560	0.145	0.538

Typical results are depicted in **Fig.2**. In addition, these results were fitted by polynomial laws as a function of x for the different inter-QD separations studied and summarized in Table.2.

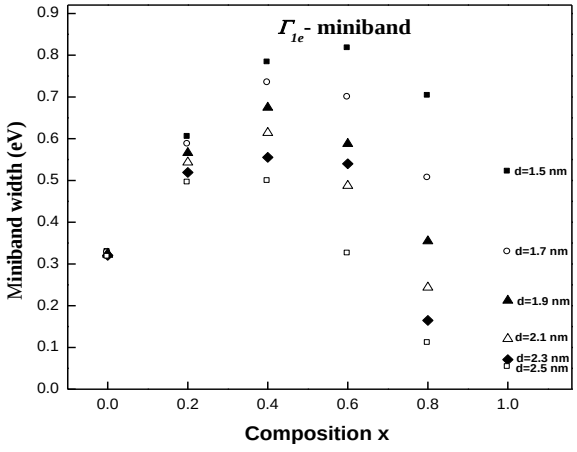

Fig.2: The Γ_1 - miniband width, as calculated for electrons versus the ZnS molar fraction for different inter-QD separations.

Table 2: The fit of the Γ_{1e} - miniband width versus the Zn composition for different inter-QD separations.

Superlattice period (nm)	Γ_{1e} – miniband
1.5	$0.324-1.813x-1.780x^2+0.158x^3$
1.7	$0.318+1.996x-2.820x^2+0.825x^3$
1.9	$0.314+2.085x-3.663x^2+0.951x^3$
2.1	$0.312+2.049x-4.097x^2+0.591x^3$
2.3	$0.306+1.876x-3.634x^2+1.489x^3$
2.5	$0.309+1.845x-4.495x^2+2.387x^3$

It was revealed that (i) for any composition x, the width ΔE_{1e} of the Γ_1 – miniband decreases with the increase of the SL period d. The coupling between nanoparticles shows a significant drop as the inter – quantum dot separation increases. This behaviour can be attributed to the fact that this coupling is governed by the tunnelling effect for shorter SL periods (ii) for larger ZnS molar fractions, the coupling is low especially for higher SL periods. In this case, $Cd_{1-x}Zn_xS$ nanocrystallites tend to behave as isolated QDs. Such a trend is due mainly to the largeness of barrier heights (iii) practically, for all the inter – quantum dot separations studied, ΔE_{1e} is shown to increase with Zn composition up to x = 0.4 and it decreases as x increases from 0.4 to 1.0. Since the effective mass m_e^* remains practically unchanged for all Zn compositions, this result is, presumably related to the barrier potential height U_{0e} and the energy E_{1e} (iv) for $Cd_{1-x}Zn_xS$ QDs with x = 0.4, the order of magnitude of the width ΔE_{1e} is important especially for shorter inter-quantum dot separations and shows the strong degree of coupling between the QDs.

For comparison with results obtained by using the Kronig-Penney, the sinusoidal and the triangular potential models [14-16], we report in Table.3, widths of Γ_1 – miniband as calculated in the present work and those obtained in Refs. [14-16]. As can be seen, practically, for all the compositions and inter- QD separations studied, the miniband widths of the present work are higher compared to those obtained by the other potential models. The reason consists on the hypothesis adopted within the Tight Binding Approximation.

Table 3: Widths of the Γ_{1e} (eV) –miniband for the present work (a) and those obtained by the triangular potential (b), the sinusoidal potential (c) and the kronig-penney potential (d).

x d (nm)	0.0	0.2	0.4	0.6	0.8	1.0
1.5	$0.328^{(a)}$	$0.604^{(a)}$	$0.782^{(a)}$	$0.816^{(a)}$	$0.702^{(a)}$	$0.520^{(a)}$
	$0.369^{(b)}$	$0.320^{(b)}$	$0.289^{(b)}$	$0.254^{(b)}$	$0.236^{(b)}$	$0.210^{(b)}$
	$0.711^{(c)}$	$0.587^{(c)}$	$0.511^{(c)}$	$0.420^{(c)}$	$0.229^{(c)}$	$0.162^{(c)}$
	$0.727^{(d)}$	$0.676^{(d)}$	$0.586^{(d)}$	$0.494^{(d)}$	$0.331^{(d)}$	$0.234^{(d)}$
1.7	$0.326^{(a)}$	$0.586^{(a)}$	$0.733^{(a)}$	$0.698^{(a)}$	$0.505^{(a)}$	$0.328^{(a)}$
	$0.286^{(b)}$	$0.251^{(b)}$	$0.224^{(b)}$	$0.198^{(b)}$	$0.146^{(b)}$	$0.163^{(b)}$
	$0.523^{(c)}$	$0.450^{(c)}$	$0.379^{(c)}$	$0.307^{(c)}$	$0.148^{(c)}$	$0.105^{(c)}$
	$0.586^{(d)}$	$0.533^{(d)}$	$0.442^{(d)}$	$0.325^{(d)}$	$0.191^{(d)}$	$0.130^{(d)}$
1.9	$0.324^{(a)}$	$0.566^{(a)}$	$0.674^{(a)}$	$0.587^{(a)}$	$0.354^{(a)}$	$0.212^{(a)}$
	$0.240^{(b)}$	$0.200^{(b)}$	$0.173^{(b)}$	$0.158^{(b)}$	$0.146^{(b)}$	$0.131^{(b)}$
	$0.449^{(c)}$	$0.335^{(c)}$	$0.292^{(c)}$	$0.230^{(c)}$	$0.091^{(c)}$	$0.055^{(c)}$
	$0.468^{(d)}$	$0.408^{(d)}$	$0.306^{(d)}$	$0.242^{(d)}$	$0.102^{(d)}$	$0.051^{d)}$
2.1	$0.322^{(a)}$	$0.543^{(a)}$	$0.614^{(a)}$	$0.487^{(a)}$	$0.243^{(a)}$	$0.120^{(a)}$
	$0.210^{(b)}$	$0.163^{(b)}$	$0.145^{(b)}$	$0.130^{(b)}$	$0.120^{(b)}$	$0.107^{(b)}$

	0.345[(c)]	0.281[(c)]	0.223[(c)]	0.165[(c)]	0.064[(c)]	0.034[(c)]
	0.370[(d)]	0.306[(d)]	0.234[(d)]	0.242[(d)]	0.065[(d)]	0.039[(d)]
2.3	0.320[(a)]	0.519[(a)]	0.555[(a)]	0.539[(a)]	0.164[(a)]	0.070[(a)]
	0.150[(b)]	0.136[(b)]	0.120[(b)]	0.108[(b)]	0.100[(b)]	0.080[(b)]
	0.276[(c)]	0.226[(c)]	0.178[(c)]	0.120[(c)]	0.044[(c)]	0.023[(c)]
	0.312[(d)]	0.250[(d)]	0.175[(d)]	0.112[(d)]	0.037[(d)]	0.012[(d)]
2.5	0.316[(a)]	0.494[(a)]	0.498[(a)]	0.324[(a)]	0.110[(a)]	0.052[(a)]
	0.130[(b)]	0.115[(b)]	0.101[(b)]	0.090[(b)]	0.080[(b)]	0.070[(b)]
	0.230[(c)]	0.190[(c)]	0.136[(c)]	0.085[(c)]	0.023[(c)]	0.009[(c)]
	0.267[(d)]	0.260[(d)]	0.153[(d)]	0.075[(d)]	0.025[(d)]	0.012[(d)]

In a second phase, we have calculated, for the heavy holes and light holes, the Γ_1 − miniband width. This parameter is denoted for these carriers by ΔE_{1hh} and ΔE_{1lh} respectively. Calculations were also carried out for the inter-sheet separations and Zn compositions studied. The parameters used are reported in Table 1. The results are depicted in Fig.3 and Fig.4. Besides, these results were fitted by polynomial laws and reported in Table 4 and Table 5.

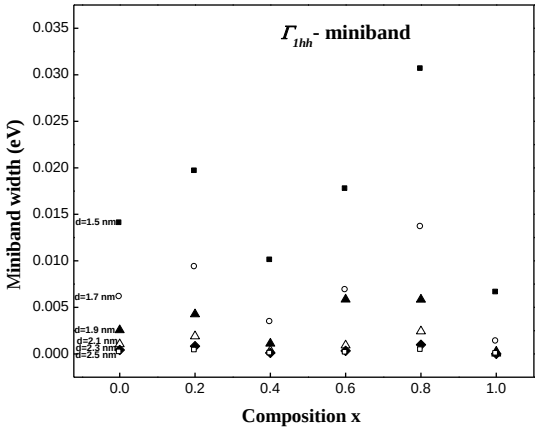

Fig.3: The Γ_1 - miniband width, as calculated for heavy holes versus the ZnS molar fraction for different inter-QD separations.

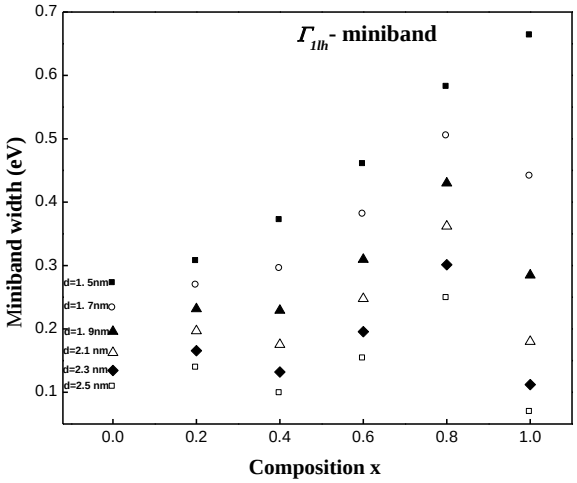

Fig.4 The Γ_1 - miniband width, as calculated for light holes versus the ZnS molar fraction for different inter-QD separations.

Table 4: The fit of the Γ_{1hh} - miniband width versus the Zn composition for different inter-QD separations.

Superlattice period (nm)	Γ_{1hh} – miniband
1.5	$0.016-0.065x+0.225x^2-0.167x^3$
1.7	$0.007-0.032x+0.105x^2-0.071x^3$
1.9	$0.003-0.015x+0.061x^2-0.048x^3$
2.1	$0.001-0.005x+0.017x^2-0.012x^3$
2.3	$5.705*10^{-4}-0.002x+0.006x^2-0.004x^3$
2.5	$2.305*10^{-4}-7.605*10^{-4}x+0.002x^20.001x^3$

Table 5: The fit of the Γ_{1lh} - miniband width versus the Zn composition for different inter-QD separations.

Superlattice period (nm)	Γ_{1lh} – miniband
1.5	$0.274-2.063*10^{-4}x+0.764x^2-0.372x^3$
1.7	$0.242-0.293x+1.603x^2-1.101x^3$
1.9	$0.210-0.459x+2.014x^2-1.465x^3$
2.1	$0.179-0.527x+2.117x^2-1.571x^3$
2.3	$0.151-0.539x+2.040x^2-1.522x^3$
2.5	$0.125-0.499x+1.834x^2-1.374x^3$

An analysis of the obtained results led to two main observations: (i) concerning the heavy holes, ΔE_{1hh} is insignificant in terms of magnitude order which means that the strong localization character of heavy holes in the SL systems is highly preserved going from CdS to ZnS independently to the inter-QD separation (ii) for the light holes, practically for all the cases studied, ΔE_{1lh} presents a maximum at x = 0.8. Moreover, ΔE_{1lh} is slightly lower than ΔE_{1e}. As a consequence, the superlattice behavior affects not only the conduction electrons but also the light holes especially for short SL periods. These results are mainly due to the difference in effective masses between the electrons and light holes on the one hand and the heavy holes on the other hand.

IV. Conclusion

We investigated the electronic properties of nanostructure based on $Cd_{1-x}Zn_xS$ embedded in a dielectric matrix for compositions ranging from CdS to ZnS. To describe the QDs, we have adopted the flattened cylindrical geometry with a finite potential barrier at the boundary. Using the Tight Binding Approximation, we have calculated, in a first phase, the Γ_1 - miniband for electrons. Calculations have been made as a function of Zn composition for different inter – quantum dot separations. An analysis of the obtained results has evidenced that the Zn composition x = 0.4 is expected to be the most favorable to give rise a superlattice behavior for the $Cd_{1-x}Zn_xS$ quantum dots studied. For heavy holes, the Γ_1 - miniband is shown to be lower in comparison with the electron miniband. This result reflects the strong localization character of heavy holes in the $Cd_{1-x}Zn_xS$ nanostructures. As for the light holes, the width magnitude order of Γ_1 - miniband is slightly lower to the one of electrons. Moreover, as has been demonstrated, the $Cd_{0.2}Zn_{0.8}S$ system is the more appropriate to exhibit a superlattice behavior for light holes especially when the superlattice period is low. In the applied physics, this study can open a way for designing a new family of nanocrystal devices based on $Cd_{1-x}Zn_xS$ QDs particularly the non – volatile memories.

References

[1] B. Bhattacharjee, S. K. Mandal, K. Chakrabarti, D. Ganguli and S. Chaudhui, J. Phys. D: Appl. Phys. 35 (2002) 2636-2642.
[2] K.K Nanda, S.N. Sarangi, S. Mohanty, S.N. Sahu, Thin Solid Films 322 (1998) 21-27.
[3] H. Yükselici, P. D. Persans and T. M. Hayes, Phys. Rev. B. 52 (1995) 11763.
[4] Y. Kayanuma, Phys. Rev. B 38 (1988) 9797
[5] L Zhou, Y Xing and Z P Wang, Eur. Phys. J. B. 85 (2012) 212
[6] A. John Peter and C. W. Lee, Chinese Phys. B 21 (2012) 087302
[7] N. Safta, A. Sakly, H. Mejri and Y. Bouazra, Eur. Phys. J. B 51 (2006) 75-78
[8] A. Sakly, N. Safta, A. Mejri, H. Mejri, A. Ben Lamine, J. Nanomater (2010), ID746520.
[9] L. Cao, S. Huang and S. E, Journal of colloid and interface science, 273 (2004) 478-482.
[10] H. Kumano, A. Ueta and I. Suemune, Physica E 13 (2002) 441-445.
[11] Y. Cai Zhang, W. Wei Chen and X. Ya Hu, Materials Letters 61 (2007) 4847-4850.

[12] K. Tomihira, D. Kim and M. Nakayama, Journal of Luminescence 112 (2005) 131-135.
[13] N. Safta, A. Sakly, H. Mejri and M. A. Zaïdi, Eur. Phys. J. B 53 (2006) 35 – 38
[14] A. Sakly, N. Safta, H. Mejri, A. Ben Lamine, J. Alloys Compd. 476 (2009) 648–652.
[15] A. Sakly, N. Safta, H. Mejri, A. Ben Lamine, J. Alloys Compd.509 (2011) 2493–2495
[16] S. Marzougui, N. Safta, IOSR-JAP 5 (5) (2014) 36-42
[17] S. Marzougui, *A study of the excited states in the flattened cylindrical quantum dots of $Cd_{1-x}Zn_xS$*, Master, University of Monastir (2011).
[18] Q. Pang, B.C. Guo, C.L. Yang, S. H. Yang, M.L. Gong, W.K. Ge and J. N. Wang, Journal of Crystal Growth, 269 (2004) 213.
[19] M.C. Klein, F. hache, D. Ricard and C. Flytzanis, Phys Rev. B. 42 (1990) 11123.